[Frontiers in Bioscience 14, 3085-3093, January 1, 2009]

Novel shear flow assay provides evidence for non-linear modulation of cancer invasion

Samuel Hagglund[1], Andreas Hoppe[1], Deborah Aubyn[2], Tamara Cavanna[2], Peter Jordan[2], Daniel Zicha[2]

[1]Kingston University, Digital Imaging Research Centre, Penrhyn Rd, Kingston-upon-Thames KT1 2EE, UK, [2]Cancer Research UK London Research Institute, Lincoln's Inn Fields Laboratories, London WC2A 3PX, UK

TABLE OF CONTENT

1. ABSTRACT

Cancer is a frequent disease in western countries and there is no effective treatment for metastasis, the main cause of death in cancer patients. The situation can be improved by a better understanding of the cancer invasion process. In order to reveal new aspects of this dynamic process, we developed a novel direct viewing cancer cell invasion assay with shear flow in vitro. This assay comprised of a custom-made flow chamber, specially developed cell labelling, high-resolution wide-field microscopy and image-processing-based quantitation. We applied this assay to metastatic rat sarcoma cells which invaded monolayers of rat endothelial cells. Our findings showed that after adhesion, the sarcoma cells initially invaded significantly faster under flow conditions compared to situations without shear stress. Later, however, the rate of invasion under flow decreased and the sarcoma cells without shear stress achieved significantly higher levels of invasion. Our observations thus revealed the non-linear modulation of a cancer cell invasion process by shear flow, demonstrating that cancer cells can respond to flow by enhancement of invasiveness similarly to white blood cells.

2. INTRODUCTION

Metastasis is still the major problem for cancer patients since it is responsible for the majority of their deaths (1) and cancer has become one of the most common diseases in western countries. The process by which metastases form is referred to as the metastatic cascade (2). In many cases of cancer, the metastatic cascade involves tumour cells spreading in the body through blood vessels. The metastatic cascade can then be described as a sequence of necessary events (3) according to Figure 1. In this metastatic cascade, the tumour cells have to actively invade through endothelium twice (intravasation and extravasation). The invasion is therefore a very important aspect of the metastatic cascade (4) and has been extensively studied.

Some of these studies were limited to static observation of the end result of the invasion process without flow using transwell chambers, such as Boyden chambers, (5-7). Honn *et al.* (8) and Li *et al.* (9) used radioactive labelling to quantify aspects of the invasion at the end of the process. Other studies without flow include: Lewalle *et al.* (10) who observed tumour induced opening

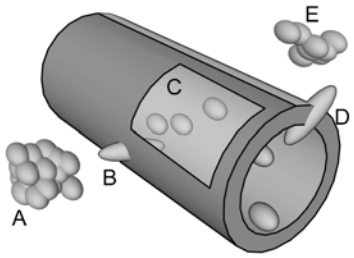

Figure 1. Diagram of the hematogenous metastatic cascade illustrating the importance of active cell migration through the endothelium. A subset of tumour cells leaves the primary tumour (A) and intravasates (B) into the blood circulation system (C). Some of those cells adhere to the vessel wall at a remote site and extravasate (D) into the surrounding tissue. Proliferation occurs once the transmigration through the endothelial cells is complete and forms the basis of a secondary tumour – metastasis (E).

of gaps between endothelial cells in monolayers by means of scanning electron microscopy at different time points; Voura *et al.* who used confocal microscopy (11) and epifluorescence microscopy (12) to classify the invasion of tumour cells into monolayers of endothelial cells using fixed specimen**;** and Hart *et al.* (13) who used time-lapse confocal microscopy and manual scoring to study the invasion of individual cells into endothelial monolayers. In order to investigate the influence of shear flow on the invasion of tumour cells Dong *et al.* developed a transwell assay (14) and applied it to score the frequency of transmigration events (15). Quantitation of cell spreading during invasion with shear flow has been manually classified and measured for the invading cells (16). Adhesion of tumour cells was also investigated under flow conditions (17-20).

We decided to explore additional aspects of the extravasation process by high-resolution 3D imaging combined with an image-processing-based quantitation of its dynamics. For this we have chosen an *in vitro* system with a flow chamber where high-resolution 3D microscopy can be achieved. One major problem, we faced in the early stages of the assay development, was cell labelling. A range of commercially available dyes and protocols did not give us sufficiently well defined labelling of cell surfaces with suitable contrast and photostability we required for the 3D quantitative analysis. Therefore we developed a modified cell labelling protocol, which overcame these problems. The image data acquired with cells labelled according to this protocol were ready for an image processing procedure, which also needed to be developed for this assay. Our approach revealed a novel aspect of the invasion process, namely its non-linear modulation by the shear flow.

3. MATERIALS AND METHODS

3.1. Cell culture

Our direct viewing assay required two cell types, sarcoma cells in suspension and endothelial cells that formed confluent monolayers.

Sarcoma cells, T15 and K2, were derived from inbred rats (21). The sarcoma cells were maintained in MEM with Hanks' salts supplemented with 10% bovine serum (SML, Germany), 0.09% sodium bicarbonate, 0.12 g/l Na-pyruvate (Sigma) and 1 mM glutamine, at 37ºC with 5% CO_2 using vented 25 cm^2 tissue culture flasks. Cells were detached from flasks by brief exposure to trypsin-versene solution (1:5) and suspended in 37°C phenol red free medium prior to recording. Cells were not used beyond passage 14.

Rat brain endothelial cells RBE4 were obtained as a kind gift from Professor Joan Abbott, Centre for Neuroscience Research, GKT School of Biomedical Sciences, King's College London, UK. Stock RBE4 cells were cultured in vented 25 cm^2 collagen coated BD BioCoat flasks (Becton Dickinson Labware, Two Oak Park, Bedford, UK) with medium containing 45% Hams F-10 (GibcoBRL), 45% alpha-MEM (GibcoBRL), 10% foetal calf serum (Sigma), 1mM Glutamax-1 (Invitrogen), 1 ng ml^{-1} bFGF (Boehringer) and 100 mg ml^{-1} Geneticin (Sigma) and then seeded at a concentration of 2 x 10^4 on 35 mm glass bottom culture dishes pre-coated with type I collagen (MatTek Corp., MA, USA). Confluency was reached after 5 days of incubation at 37ºC with 10% CO_2. Early experimentation suggested that higher seeding densities lead to confluency in a shorter time period (e.g. 2 to 3 days), but the resulting layer did not remain intact under flow. A period of 5 days was established as being a suitable time period for strong cell adherence under flow conditions.

3.2. Cell labelling

The sarcoma cells were labelled with 10 uM green Vybrant DiO solution (Invitrogen, USA). We chose this dye because it has good photostability and produces high intensity fluorescent signal. Although the intracellular distribution is predominantly punctate, we were able to use it as volume indicator since there is some diffuse staining and the puncta are distributed throughout the cytosol. The supplied solution was diluted in 2 ml of the culture medium then placed into a nearly confluent flask with approximately 2 x 10^6 sarcoma cells, which were subsequently incubated for 15 min at 37°C. The cells were then washed with pre-warmed medium and trypsinised. The sarcoma cells were then suspended in phenol red free medium ready to be introduced into the flow chamber.

The endothelial cells were labelled by a new protocol we developed using CellTracker Orange CMTMR (Invitrogen Ltd). The protocol is described in the Results section.

3.3. Flow chamber

We developed a custom-made flow chamber for the direct viewing assay as described in the Results section. The chamber design incorporated a 35 mm glass bottom MatTek dish (MatTek Corp., MA, USA) as shown in Figure 2.

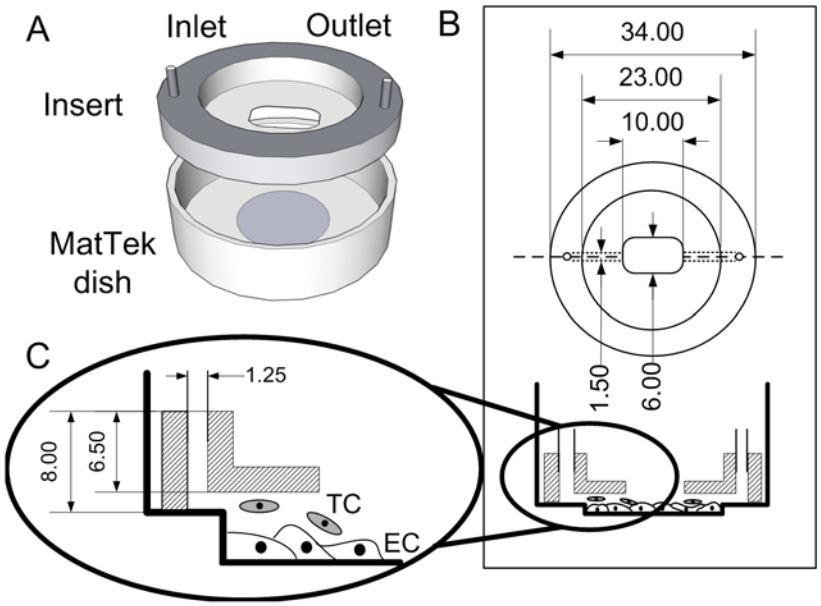

Figure 2. Schematic drawing of our flow chamber. The custom-made Nylon insert fits into a MatTek dish with a confluent monolayer of endothelial cells (EC). The cells are exposed to the shear stress in an oval aperture in the centre of the insert. This central aperture is open and allows initial introduction of tumour cells (TC). The entire flow chamber is presented in 3D (A) and as top-view/cross-section (B). Detail view (C) depicts the vertical inlet tube, which is connected to the central aperture by a channel cut into the base of the insert using a milling machine. A symmetrical channel connects the opposite end of the central aperture to the outlet tube. On the outside the outlet is connected to the inlet by flexible tubing going through a peristaltic pump. Measurement units are in mm**.**

For calibration, the shear force P in the flow chamber was calculated using Equation 1,

$$P = e\frac{d}{t \cdot h} \qquad (1)$$

where the dynamic viscosity of the culture medium e was taken to be 0.653 mN s m^{-2}. A particle flowing through the chamber, at the height h of 8 um above surface, was used to measure the flow speed by determining its travel distance d of 50 um over the observation time t of 277 ms. The shear force P was calculated to be 14.7 dynes cm^{-2}. This fairly high shear force was chosen to give us a good contrast between no flow and flow conditions, while still lying within the range used in previous studies, such as (16).

3.4. Microscopy and image acquisition

The custom-made flow chamber with labelled endothelial monolayer was connected to a peristaltic pump by flexible tubing to form a circulation system. The chamber was secured into a 35 mm culture dish stage insert and placed onto the microscope stage within a 37°C temperature controlled enclosure. Since the endothelial cells may change shape and compromise confluency when flow is started for the first time, shear flow was applied for an interval of 15 min before choosing 20 confluent observation fields based on visual inspection of the labelled endothelial cells. The fields were selected for subsequent multi-field recording in the MetaMorph (Universal Imaging Corp, USA) software for acquisition of images using a 60x 1.45 NA lens on a Nikon TE2000 inverted wide-field microscope, equipped with a scientific cooled CCD camera (Cascade-II, Photometrics), fluorescence filter wheels (Lambda 10-3, Sutter) and a motorised stage (MS2000, ASI). After the field selection which took about 5 min, the acquisition was started and each field was revisited every 15 min acquiring image z-stacks of both the sarcoma cells and the endothelial cells. Stacks of 21 images were acquired with 1 um z-step using binning 2, which provided a 0.2 um x 0.2 um x 1 um voxel (volume-element) size. The wavelength of the excitation light alternated between the z-stacks using 488 nm for imaging of the sarcoma cells labelled with green fluorescence, and 540 nm for imaging of the endothelial cells labelled with orange fluorescence. The suspended labelled sarcoma cells were introduced into the central aperture of the chamber immediately after the first acquisition time point. The peristaltic pump was then switched on at the second time point, and left to constantly circulate medium. Image stacks were acquired every 15 min for 90 min at each field.

Control experiments without flow were performed in MatTek dishes using identical imaging configuration. Paired experiments without flow and with flow were repeated three times for metastatic sarcoma cells T15. Non-metastatic cells K2 were assessed twice under conditions without flow.

We also used a laser scanning confocal microscope LSM 510 (Carl Zeiss MicroImaging GmbH, Jena, Germany) with 63x 1.4 NA lens for imaging cells

fixed with 4% paraformaldehyde solution in order to complement the dynamic studies.

3.5. Image-processing-based quantitative analysis of invasion

We developed two new measurement parameters, Relative Invasion and Opening Rate of the Endothelial Monolayer, to quantify the invasion of sarcoma cells into monolayers of endothelial cells.

The Relative Invasion (*RI*) parameter was defined as the sum of the z-projected intensities of the green fluorescence signal inside an invading sarcoma cell below the upper monolayer surface divided by the sum of the z-projected intensities throughout the entire image stack of the sarcoma cell as described in Equation 2.

$$RI = \frac{\sum_{<x,y>\in\Omega_I} \mathrm{Proj}_I(x,y)}{\sum_{<x,y>\in\Omega_C} \mathrm{Proj}_C(x,y)} \qquad (2)$$

where

$$\mathrm{Proj}_I(x,y) = \underset{z=1}{\overset{U(x,y)}{Max}}(I(x,y,z)),\ \mathrm{Proj}_C(x,y) = \underset{z=1}{\overset{top}{Max}}(I(x,y,z)),$$

$omega_I$ is a set of N positions <x,y> of an invading sarcoma cell with signal in the z-projection below the upper endothelial monolayer surface *U (x,y)* and $omega_C$ is a set of N positions <x,y> with signal in the z-projection of the whole image stack. *I (x,y,z)* denotes the signal of a 3D volume element (voxel) in the image stack. The *RI* parameter was calculated only for a subset of cells selected for sufficiently strong fluorescence signal and well-defined separation from neighbouring cells. In control experiments 9 out of 104 cells and in flow experiments 13 out of 111 cells were selected manually. In order to determine the positions ($omega_I$ or $omega_C$) with cell signal of an invading sarcoma cell in the projection images, we used linear diffusion (22) to separate cell signal from out-of-focus blur. Linear diffusion was applied to the projection images by blurring it consecutively with a 2D Gaussian filter of 11 x 11 pixels (sigma = 0.5) for 20 iterations. With each iteration, cell signal intensities were more diffused. The rates at which the signal intensities diffused were different from the rates of out-of-focus blur intensity diffusion. To obtain the cell signal in the projection images we calculated a threshold by a variant of the SURE procedure (23) on the total intensity projection Proj_C. The same threshold was applied to the projection image below the surface Proj_I. Only signal intensities with diffusion rates above the calculated threshold were considered part of the cell as described previously (24). To obtain the upper surface of the endothelial monolayer *U (x,y)*, a new surface reconstruction technique was developed which calculates the in-focus level of each <x,y> pixel position from wide-field image stacks. To emphasise high contrast features located on the cell surface, a high pass filter (i.e. gradient filter) was applied to each image z-plane. A surface level was determined at each <x,y> position by the highest axial gradient value in the z-stack. The surface levels in an image were represented as a 2D depth map which was post-processed with a 5 x 5 median filter to remove noise. At the invaded areas with absence of the signal from the upper surface of the endothelial cells, we interpolated the surface. In order to identify these areas, we applied linear diffusion on the minimum projection image of the endothelial z-stack by convolving the projection image with a 2D Gaussian kernel of 11 x 11 pixels (sigma = 0.5) for 500 iterations consecutively. In the minimum projection image, the diffusion rates of signal values were negative while the diffusion rates of invaded areas were positive. Thus, we could identify regions that required surface interpolation. To interpolate the surface over the invaded areas, we applied a radial basis function interpolation approach (25). Surface surrounding invaded areas provided the vertices for the interpolating function.

The Opening Rate of the Endothelial Monolayer (*OREM*) was measured during invasion by quantifying the reduction of the fluorescence signal of the endothelial cells in a 4 um x 4 um area where invasion commenced. The location of an area was selected manually for each cell and remained the same over time. The signal was measured from the minimum projection of the image z-stacks of monolayer cells for each time point. The sarcoma cell-induced opening in the monolayer resulted in a decrease of signal value over time in the selected areas of the minimum projection images. The intensity of the projection images *I* was normalised (Equation 3) over the monitoring period of 90 min and thus comparable between repeated experiments.

$$I_{norm}(t) = \frac{I(t) - \min(I)}{\max(I) - \min(I)} \qquad (3)$$

OREM was calculated as the difference of the normalised intensities at invasion positions between the two time points: t_1 = 0 min and t_2 = 30 min (Equation 4).

$$OREM = I_{norm}(t_1) - I_{norm}(t_2) \qquad (4)$$

All image processing functions were custom developed in MATLAB R14 (The Mathworks Ltd., UK).

4. RESULTS

4.1. Novel flow chamber assay with image-processing-based measurements designed for studying the dynamics of the invasion of sarcoma cells into monolayers of endothelial cells

Our direct viewing assay used a flow chamber with a custom-made Nylon insert fitting tightly into a 35 mm glass bottom MatTek dish as shown in Figure 2. Such a design allowed for convenient cell culturing of the monolayer and assembly of the chamber. The glass bottom dish enabled the specimen to be viewed in high-resolution fluorescence microscopy. The chamber had an inlet and outlet, a flow channel and an aperture in the centre to allow for easy introduction of sarcoma cells in suspension. The

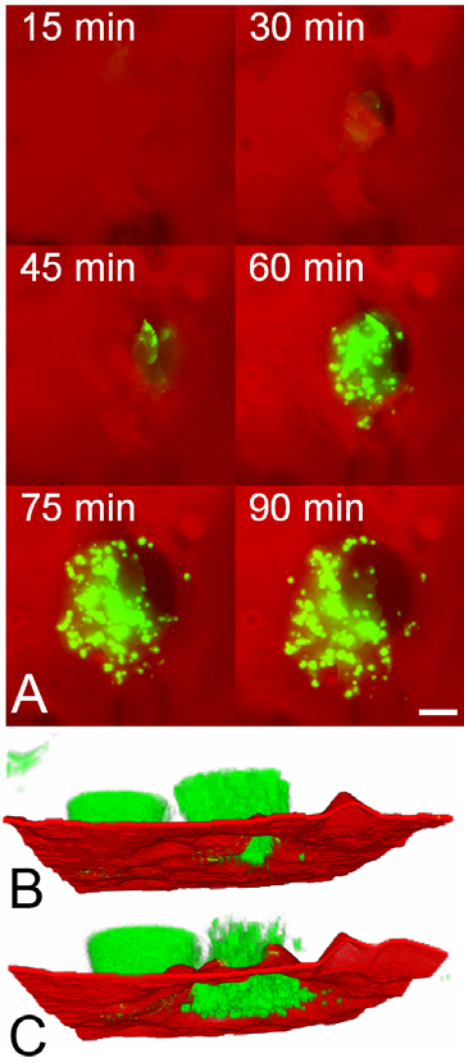

Figure 3. Images illustrating sarcoma cells invading monolayers of endothelial cells. Endothelial cells labelled with CellTracker Orange CMTMR, using our novel protocol, are represented in red and sarcoma cells labelled with Vybrant DiO solution are represented in green. The Vybrant DiO dye produces punctate staining throughout the cytosol. (A) presents images from a time-lapse recording of a sarcoma cell invading a monolayer of endothelial cells. Images of the endothelial cells show minimum z-projections and images of the sarcoma cell show maximum z-projections of optical sections obtained between the surface of the monolayer and the substrate. The invasion was monitored over 90 min and the sarcoma cell was found to partially extend under the monolayer after 30 min. Scale bar represents 5 um. (B) and (C) show 3D-reconstructions, at early and late stages of invasion respectively, of an adhering sarcoma cell (left) and an invading sarcoma cell (right) interacting with a monolayer of endothelial cells. The raw data were acquired as stacks of wide-field images. The surface of the endothelial cells was reconstructed by locating the in-focus level at each <x,y> position. The images of the sarcoma cells were processed by high-pass filtering and soft thresholded to reduce out of focus blur. The images were pre-processed by custom developed software in MATLAB and the resulting data were presented using Volocity (Improvision Inc).

inlet and outlet were connected to a peristaltic pump to provide shear flow in the chamber.

Cell labelling was a crucial component of this direct viewing assay. Sarcoma cells were labelled with 10 uM green Vybrant DiO solution (Invitrogen Ltd) according to a protocol provided by the manufacturer. In order to assess the invasion by sarcoma cells, it was necessary to label the surface membrane of the endothelial cells uniformly and specifically without significant internalisation and cross-leakage to the invading sarcoma cells for long time periods. In order to meet these requirements, we developed a new labelling procedure for a commercially available cell dye, CellTracker Orange CMTMR (Invitrogen Ltd). The labelling reagent was diluted to a 100 uM concentration in high-quality DMSO (Sigma), aliquoted into 100 ul units and kept at -20°C for at least 2 weeks before use. We empirically found that the 2 week period was essential for achieving the improved labelling. 30 ul of the prepared reagent was added to the adherent monolayer of endothelial cells in a MatTek dish containing 2 ml of culture medium and mixed using a pipette. The adherent cells were then incubated for 5 min at 4°C and subsequently washed twice with pre-warmed medium and incubated for another 15 min at 37°C. This technique provided prolonged photostability and excellent definition of the endothelial cell monolayer surface.

We devised two new imaging-based parameters to quantify the invasion process using z-stacks of images of labelled cells in the flow chamber acquired by time-lapse fluorescence microscopy. The first parameter, *RI*, measured the penetration of the monolayer of endothelial cells by a sarcoma cell. The *RI* parameter was calculated as the ratio of the sum of the projected signal of an invading sarcoma cell below the upper monolayer surface over the total projection signal in the stack of sarcoma cell images. This required a signal in the sarcoma cells as well as the reconstructed surface over the invaded area on the monolayer of endothelial cells. Image stacks were acquired at 1 um z-distance, which did not meet the Nyquist criterion and standard deconvolution approach did not produce acceptable results. Instead, we applied linear diffusion to separate the signal in z-stacks of images from the out of focus blur. The surface of the monolayer was determined by calculating the in-focus level from the high-pass filtered image stack. An example of a reconstructed surface is shown in Figure. 3B and 3C. The surface in areas without fluorescent signal, i.e. invaded areas, was reconstructed by 2D radial basis function interpolation, which interpolated over gaps in the monolayer. This was necessary to determine which part of an invading sarcoma cell was above and below the monolayer surface.

To validate the calculation of the *RI* parameter, 12 cells (6 from flow and 6 from control experiments) were selected randomly. For each cell ellipses were drawn around the outline at each z-plane throughout the cell

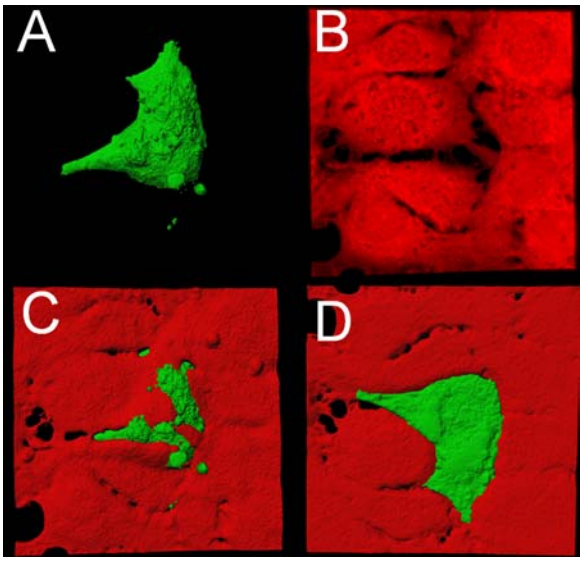

Figure 4. Images of a sarcoma cell invading a monolayer of endothelial cells without flow where the sarcoma cell had invaded almost completely underneath the surface of the monolayer. The images present renderings of a z-stack of images (field size 73 um x 73 um) acquired from 50 z-levels at 0.2 um separation by a laser scanning confocal microscope LSM 510 (Carl Zeiss MicroImaging GmbH, Jena, Germany). Endothelial cells labelled with CellTracker Orange CMTMR were imaged using a 543 nm line of a HeNe laser and are represented in red, and the sarcoma cell labelled with green DiO was imaged using a 488 nm line of an Argon laser and is represented in green. (A) Shows the isosurface rendering of the sarcoma cell. (B) presents the maximum intensity projection of the endothelial monolayer where the individual cells and gaps between them can be identified. (C) and (D) show the top view and the bottom view of combined isosurfaces. The images were rendered using Imaris (Bitplane AG, Switzerland).

height. The areas of the ellipses were integrated over the z-stack to approximate cell volume. Relative invasion volume was calculated as the volume underneath the upper surface of the endothelial cells divided by the entire cell volume. The upper surface of the endothelial cells, in this case, was found by inspecting the stack manually for the in-focus position. The calculated *RI* values from our image-processing-based approach and the manually determined relative invasion volumes correlated well (Pearson correlation coefficient r = 0.89) and showed significance in linear regression analysis (P-value < 0.005).

The second parameter, *OREM* quantified the change of the fluorescent signal of the endothelial cells in a 4 um x 4 um area where invasion occurred. In this area, the signal was measured from the minimum projection of the image z-stacks of endothelial cells for each time point. The decreasing intensity was normalised over the monitoring period and thus comparable with other experiments.

4.2. Metastatic sarcoma cells invade the monolayer of endothelial cells by opening gaps between endothelial cells while non-metastatic sarcoma cells do not

The newly developed invasion assay was used to study the invasion of metastatic rat sarcoma cells T15 into monolayers of rat brain endothelial cells over a time period of 90 min. We observed the sarcoma cells invading the monolayer by inducing gaps between the endothelial cells from as early as 15 min after initial adherence to the monolayer. The invading sarcoma cells extended underneath the surface of the monolayer (Figure. 3A). An example of a 3D-reconstruction of an adhering sarcoma cell and an invading sarcoma cell interacting with a monolayer of endothelial cells is shown in Figure 3B and Figure 3C. Sarcoma cells were also observed to have almost completely invaded underneath the surface of the monolayer as shown in the 3D-rendering of confocal images in Figure 4.

In addition we applied the invasion assay to compare the invasion potential of another sarcoma cell population K2. It was previously reported from *in vivo* experiments that the T15 sarcoma cells have a significantly higher metastatic potential compared to the non-metastatic K2 sarcoma cells (26). Using our direct viewing invasion assay, we observed that there was no invasion into the monolayer of endothelial cells by the non-metastatic K2 sarcoma cells in two experiments without flow.

4.3. The initial invasion rate of the metastatic cells is enhanced by shear flow while later the cells without shear stress achieve higher levels of invasion

To quantitatively assess the invasion process, we calculated *RI* values for the invading sarcoma cells. Figure 5 shows a graph of *RI* values plotted as connected data points for control experiments and flow experiments with shear stress over 90 min observation period. Sarcoma cells without shear flow exhibited lower mean invasion in the first 30 min compared to sarcoma cells exposed to shear flow. After 30 min, the situation changed and the sarcoma cells without flow eventually showed significantly higher levels of invasion in comparison to the sarcoma cells exposed to shear flow. Mean +/- standard error values of *RI* at 90 min time point were 0.6226 +/- 0.0408 (N = 9) for no flow and 0.4430 +/- 0.0432 (N = 13) for flow condition (Mann-Whitney P-value < 0.014). This indicated that shear flow stimulated the sarcoma cell invasion in the early stages but the sarcoma cells could not sustain this activity over long periods. The level of invasion significantly decreased during prolonged exposure to shear flow in comparison with the control situation without flow.

To assess whether shear flow influenced significantly the initial part of the invasion process, i.e. the opening of gaps, the *OREM* parameter was calculated for the time interval between 0 and 30 min after the acquisition began. Sarcoma cells exposed to shear flow expressed overall higher *OREM* compared to sarcoma cells without shear flow. The incidence of sarcoma cells with high (=> 0.5) and low (< 0.5) *OREM* values are shown in Table 1. In the 3 paired experiments, the incidence of sarcoma cells with high *OREM* was significantly increased under shear

Table 1. The incidences of sarcoma cells with low (< 0.5) and high (>= 0.5) opening rates of the endothelial monolayer (*OREM*) under conditions without and with shear flow from three paired experiments

***OREM* value**[1]	**low**	**high**
Incidences without flow[2]	60	44
Incidences with flow[2]	35	76

[1]The *OREM* values were calculated from data acquired at 0 and 30 min time points in the experiments using a total number of 104 cells without flow and 111 cells with flow. [2]The incidence of sarcoma cells with high *OREM* was significantly higher under shear flow (Chi^2 P-value < 0.005).

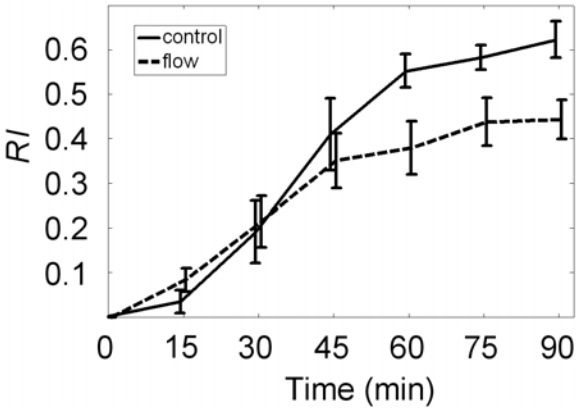

Figure 5. Relative Invasion (*RI*) of invading sarcoma cells without and with shear flow plotted over a 90 min observation period. *RI* measures the ratio of the sum of the projected signal of an invading sarcoma cell below the upper monolayer surface and the total signal in the stack of the sarcoma cell images. *RI* values are plotted as data points connected by solid lines (no shear flow) and dashed lines (flow with shear stress). Sarcoma cells without shear flow exhibited lower mean *RI* in the first 30 min compared to sarcoma cells exposed to shear flow. The significant difference of the invasion rate at this early stage is described in Table 1. Later on, the situation reversed and the sarcoma cells without flow showed a significantly higher level of invasion in comparison to the sarcoma cells exposed to shear flow. Graph represents data from 9 cells without flow and 13 cells under flow conditions. Error bars represent standard errors of the mean.

low (Chi^2 P-value < 0.005) compared to a situation without flow.

5. DISCUSSION

In this study, we developed a novel direct viewing flow assay and applied it to an investigation of metastatic rat sarcoma cells invading monolayers of rat brain endothelial cells *in vitro*. We found that the sarcoma cells exposed to shear flow expressed a significantly higher rate of invasion after the first contact with the endothelial monolayer compared with sarcoma cells not exposed to shear flow. However after 30 min the sarcoma cells with no shear forces exhibited higher levels of invasion eventually achieving significant differences.

Dong *et al. (*15) reported a decreasing number of invading tumour cells exposed to shear forces in relation to situations with no shear using transwell assays with counting the cells that had invaded. Although we also observed a reduction of invasion with our sarcoma cells at later time points, we showed that the flow can stimulate the metastatic sarcoma cells to higher rates of invasion similarly to white blood cells, such as neutrophil leucocytes (27) and lymphocytes (28). This observation can be explained by shear stress initially activating signalling pathways, which induce changes in cell motile behaviour. This proposed hypothesis is supported by some reports. Chotard-Ghodsnia *et al.* (16) used time-lapse fluorescence microscopy to manually classify and measure the tumour cells interacting with endothelial cells under shear forces and concluded that the extend of tumour cell spreading was increased by shear flow similarly to leukocytes which increased pseudopodia activity while exposed to flow (29). Changes in endothelial polarisation and migration in response to shear stress were also described by Wojciak-Stothard *et al.* (30). In addition, esophageal tumour cells expressed a similar behaviour where shear forces increased the lamellipodia activity compared to no shear (31). Furthermore, the authors reported an increase in the invasiveness of these tumour cells using a Boyden chamber assay after cells had been pre-exposed to shear flow. In their study, cells were not exposed to shear flow during the invasion process. Signalling pathway activation by mechanical forces was also reported by Bershadsky *et al.* (32) who found induction of DNA synthesis as a consequence. Our assay showed that the higher rate of the invasion process is not sustained under flow, which indicates that the shear stress activated signalling may be transient. The fact that the cells under control conditions without flow eventually achieve higher invasion might be explained by a gradual accumulation of more proteolytic enzymes in their local microenviroment than under flow conditions. This is a plausible explanation since proteolytic activity was shown to be increased in the metastatic cells T15 compared to the non-metastatic cells K2 (33) and has been shown to play a general role in invasion and metastasis (34, 35).

In previous studies, the effect of shear flow on the invasion process was quantified by means of counting and/or manual quantification of the cells that had invaded in transwell (14, 15) or parallel plate chambers (16). Our flow chamber invasion assay allowed the analysis of invading tumour cells in high-resolution 3D widefield microscopy using image-processing-based quantitation. We were able to assess the invasion process under flow conditions right from the moment shear flow was applied. The endothelial cell surface reconstruction enabled the quantitation of the levels of invasion from the signal of the invading sarcoma cells at consecutive time points. We observed sarcoma cells to invade the endothelial monolayer by opening gaps between endothelial cells. Our observations were also evaluated through our second measurement parameter, the Opening Rate of the Endothelial Monolayer. The evaluation of the two image-processing-based parameters in combination revealed the non-linear invasion response of sarcoma cells to shear stress.

The time of the initiation of the invasion we observed is similar to what other people observed in related processes. Peng *et al.* (5) reported that human melanoma cells begin the opening of gaps in the endothelial monolayer after 45 min and Lewalle *et al.* (10) observed the invasion through opening of gaps between endothelial cells after 30 min. Experiments *in vivo* show that rat colon carcinoma cells adhere 15 min after intravenous injection (36).

We described a development of a novel direct viewing flow assay on the basis of live cell imaging and new quantitative image analysis techniques. With this assay we were able to measure the invasion of individual sarcoma cells into monolayers of endothelial cells exposed to shear flow. We found that cells from a non-metastatic population were not able to invade into the endothelial monolayer. Experiments with the metastatic cells showed that shear forces significantly increased the initial sarcoma-induced invasion into the monolayers of endothelial cells. The invasion of sarcoma cells under flow conditions expressed a non-linear behaviour whereby the rate of invasion increased initially but later decreased over time compared to a situation without shear. This shows that metastatic cancer cells can be stimulated to enhance extravasation by shear flow similarly to white blood cells.

6. ACKNOWLEDGEMENTS

This work has been funded by the EPSRC Grant GR/S34250/01 and Cancer Research UK London Research Institute. We would like to thank Nancy Hogg and Alastair Nicol, Cancer Research UK London Research Institute, for comments to the manuscript.

7. REFERENCES

1. Ahmad A, I. R. Hart: Mechanisms of metastasis. *Crit Rev Oncol Hematol* 26, 163-173 (1997)

2. Meyer T, I. R. Hart: Mechanisms of tumour metastasis. *Eur J Cancer* 34, 214-221 (1998)

3. Liotta L. A: Cancer cell invasion and metastasis. *Sci Am* 266, 54-59, 62-63 (1992)

4. Fidler I. J: Critical factors in the biology of human cancer metastasis: twenty-eighth GHA Clowes memorial award lecture. *Cancer Res* 50, 6130-6138 (1990)

5. Peng H. H, L. Hodgson, A. J. Henderson, C. Dong: Involvement of phospholipase C signaling in melanoma cell-induced endothelial junction disassembly. *Front Biosci* 10, 1597-1606 (2005)

6. Tremblay P. L, F. F. Auger, J. Huot: Regulation of transendothelial migration of colon cancer cells by E-selectin-mediated activation of p38 and ERK MAP kinases. *Oncogene* 25, 6563-6573 (2006)

7. Roche Y, D. Pasquier, J. J. Rambeaud, D. Seigneurin,, A. Duperray: Fibrinogen mediates bladder cancer cell migration in an ICAM-1-dependent pathway. *Thromb Haemost* 89, 1089-1097 (2003)

8. Honn K, D. Tang, I. Grossi, Z. Dnniec, J. Timar, C. Renaud, M. Leithouser, I. Blair, C. Johnson, C. Diglio, V. Kimler, J. lhylor, L. Marnett: Tumor Cell-derived 12 (S)-Hydroxyeicosatetraenoic Acid Induces Microvascular Endothelial Cell Retraction. *Cancer Res* 54, 565-574 (1994)

9. Li Y. H, C. Zhu: A modified Boyden chamber assay for tumor cell transendothelial migration *in vitro*. *Clin Exp Metastasis* 17, 423-429 (1999)

10. Lewalle J. M, K. Bajou, J. Desreux, M. Mareel, E. Dejana, A. Noel, J. M. Foidart: Alteration of Interendothelial Adherens Junctions Following Tumor Cell-Endothelial Cell Interaction *in vitro*. *Exp Cell Res* 237, 347-356 (1997)

11. Voura E. B, M. Sandig, V. I. Kalnins, C. H. Siu: Cell shape changes and cytoskeleton reorganization during transendothelial migration of human melanoma cells. *Cell Tissue Res* 293, 375-387 (1998)

12. Voura E. B, R. A. Ramjeesingh, A. M. P. Montgomery, C. H. Siu: Involvement of Integrin avß3 and Cell Adhesion Molecule L1 in Transendothelial Migration of Melanoma Cells. *Mol Biol Cell* 12, 2699-2710 (2001)

13. Hart C. A, M. Brown, S. Bagley, M. Sharrard, N. W. Clarke: Invasive characteristics of human prostatic epithelial cells: understanding the metastatic process. *Br J Cancer* 92, 503-512 (2005)

14. Dong C, M. J. Slattery, B. M. Rank, J. You: *In vitro* Characterization and Micromechanics of Tumor Cell Chemotactic Protrusion, Locomotion, and Extravasation. *Ann Biomed Eng* 30, 344-355 (2002)

15. Dong C, M. Slattery, S. Liang: Micromechanics of tumor cell adhesion and migration under dynamic flow conditions. *Front Biosci* 10, 379-384 (2005)

16. Chotard-Ghodsnia R, O. Haddad, A. Leyrat, A. Drochon, C. Verdier, A. Duperray: Morphological analysis of tumor cell/endothelial cell interactions under shear flow. *J Biomech* 40, 335-344 (2007)

17. Giavazzi R, M. Foppolo, R. Dossi, A. Remuzzi: Rolling and adhesion of human tumor cells on vascular endothelium under physiological flow conditions. *J Clin Invest* 92, 3038-3044 (1993)

18. Haier J, M. Y. Nasralla, G. L. Nicolson: ß1-integrin-mediated dynamic adhesion of colon carcinoma cells to extracellular matrix under laminar flow. *Clin Exp Metastasis* 17, 377-387 (1999)

19. Kitayama J, N. Tsuno, E. Sunami, T. Osada, T. Muto, H. Nagawa: E-selectin can mediate the arrest type of adhesion of colon cancer cells under physiological shear flow. *Eur J Cancer* 36, 121-127 (2000)

20. Burdick M. M, J. M. McCaffery, Y. S. Kim, B. S. Bochner, K. Konstantopoulos: Colon carcinoma cell glycolipids, integrins, and other glycoproteins mediate adhesion to HUVECs under flow. *Am J Physiol-Cell Ph* 284, 977-987 (2003)

21. Pokorna E, P. W. Jordan, C. O'Neill, D. Zicha, C. Gilbert, P. Veselý: Actin cytoskeleton and motility in rat sarcoma cell populations with different metastatic potential. *Cell Motil Cytoskeleton* 28, 25-33 (1994)

22. Koenderink J. J: The structure of images. *Biol Cybern* 50, 363-370 (1984)

23. Donoho D, I. Johnstone: Adapting to Unknown Smoothness Via Wavelet Shrinkage. *J Am Stat Assoc* 90, 1200-1224 (1995)

24. Baradez M. O, C. P. McGuckin, N. Forraz, R. Pettengell, A. Hoppe: Robust and automated unimodal histogram thresholding and potential applications. *Pattern Recogn* 37, 1131-1148 (2004)

25. Carr J. C, W. R. Fright, R. K. Beatson: Surface interpolation with radial basis functions for medical imaging. *IEEE Trans Med Imag*

16, 96-107 (1997)

26. Cavanna T, E. Pokorna, P. Vesely, C. Gray, D. Zicha: Evidence for protein 4.1 B acting as a metastasis suppressor. *J Cell Sci* 120, 606-616 (2007)

27. Cinamon G, V. Shinder, R. Shamri, R. Alon: Chemoattractant Signals and ß2 Integrin Occupancy at Apical Endothelial Contacts Combine with Shear Stress Signals to Promote Transendothelial Neutrophil Migration 1. *J Immunol* 173, 7282-7291 (2004)

28. Cinamon G, V. Shinder, R. Alon: Shear forces promote lymphocyte migration across vascular endothelium bearing apical chemokines. *Nat Immunol* 2, 515-522 (2001)

29. Coughlin M.F, G. W. Schmid-Schonbein: Pseudopod Projection and Cell Spreading of Passive Leukocytes in Response to Fluid Shear Stress. *Biophys J* 87, 2035-2042 (2004)

30. Wojciak-Stothard B, A. J. Ridley: Shear stress-induced endothelial cell polarization is mediated by Rho and Rac but not Cdc42 or PI 3-kinases. *J Cell Biol* 161, 429-439 (2003)

31. Lawler K, E. Foran, G. O'Sullivan, A. Long, D. Kenny: Mobility and invasiveness of metastatic esophageal cancer are potentiated by shear stress in a ROCK-and Ras-dependent manner. *Am J Physiol-Cell Ph* 291, 668-677 (2006)

32. Bershadsky A. D, N. Q. Balaban, B. Geiger: Adhesion-dependent cell mechanosensitivity . *Annu Rev Cell Dev Biol* 19, 677-695 (2003)

33. Krepela E, P. Vesely, A. Chaloupkova, D. Zicha, P. Urbanec, D. Rasnick, J. Vicar: Cathepsin B in cells of two rat sarcomas with different rates of spontaneous metastasis. *Neoplasma* 36, 529-540 (1989)

34. Hart C. A, L. J. Scott, S. Bagley, A. A. Bryden, N. W. Clarke, S. H. Lang: Role of proteolytic enzymes in human prostate bone metastasis formation: *in vivo* and *in vitro* studies. *Br J Cancer* 86, 1136-1142 (2002)

35. Wolf K, I. Mazo, H. Leung, K. Engelke, U. H. von Andrian, E. I. Deryugina, A. Y. Strongin, E. B. Brocker, P. Friedl: Compensation Mechanism in Tumor Cell Migration: Mesenchymal-Amoeboid Transition after Blocking of Pericellular Proteolysis. *J Cell Biol* 160, 267-277 (2003)

36. Schluter K, P. Gassmann, A. Enns, T. Korb, A. Hemping-Bovenkerk, J. Holzen, J. Haier: Organ-Specific Metastatic Tumor Cell Adhesion and Extravasation of Colon Carcinoma Cells with Different Metastatic Potential. *Am J Pathol* 169, 1064-1073 (2006)

Abbreviations: *OREM*: Opening Rate of the Endothelial Monolayer; *RI*: Relative Invasion; MEM: minimal essential medium; bFGF: basic fibroblast growth factor; CMTMR: M 5- (and-6)- (((4-chloromethyl)benzoyl)amino) tetramethylrhodamine; DMSO: dimethyl sulfoxide; CCD: charge-coupled device

Key Words: Cancer metastasis, flow chamber, transmigration, extravasation, invasion assay *in vitro*, shear stress, shear flow, quantitative image processing, cell labelling

Send correspondence to: Daniel Zicha, Cancer Research UK London Research Institute, Lincoln's Inn Fields Laboratories, London WC2A 3PX, UK, Tel**:** 44-0-20 7269 3563, Fax: 44-0-20 7269 2869, E-mail**:** daniel.zicha@cancer.org.uk

http://www.bioscience.org/current/vol14.htm